

## Seismic lithostratigraphy of deep subsalt Permo-Carboniferous gas reservoirs, Northwest German Basin

M. E. Mathisen\* and M. Budny\*

### ABSTRACT

Recent improvements in land seismic data quality have made it possible to initiate lithostratigraphic interpretations of deep (4000–5500 m; 2.2–2.8 s) subsalt Permo-Carboniferous gas reservoirs in the Northwest German Basin. The first modeling and interpretation results indicate that the reflection character of Permian reservoir dolomites and sandstones can be interpreted to predict lithology and porosity variations using reflection character analysis. These formations are commonly thick enough to be resolved (>20 m) and typically have velocities 1000 to 2000 m/s slower than overlying and underlying nonreservoir rocks.

Deeper Upper Carboniferous reservoir sandstones occur within a discontinuous low-amplitude seismic facies which can be clearly differentiated from a continuous high-amplitude facies formed by the less prospective Upper Carboniferous coal measures.

The accuracy of Permian reflection character interpretations is dependent on the availability of high-frequency, zero-phase, relative amplitude seismic data. New 3-D data are appropriate but of limited availability. To provide suitable 2-D data, wavelet processing of selected variable vintage lines was completed. More routine use of wavelet processing and lithostratigraphic interpretation methods should help to better define reservoir facies and stratigraphic traps, lower prospect risk, and increase success ratios.

### INTRODUCTION

Exploration in the Northwest German Basin, the most important gas-producing basin in Germany, is focused on 4000 to 5500 m deep Permo-Carboniferous reservoirs sourced by the Upper Carboniferous coal measures and sealed by Upper Permian evaporites (Schott, 1982; Schroeder, 1986). Structural traps are commonly delineated using the base Zechstein unconformity reflection, a difficult task in many areas due to poor land seismic data quality, structural complexity, and lateral variations in velocity. Little effort has been made to interpret Permo-Carboniferous reservoir stratigraphy, lithology or porosity with seismic methods because of the limited subsalt data quality and structurally oriented acquisition and processing procedures.

Recent improvements in land seismic acquisition and processing have led to the recognition of mappable subsalt reflections and/or seismic facies. Reprocessing or wavelet-processing efforts have been necessary, in most cases, to enhance Permian and Carboniferous events and preserve

relative amplitudes. Subsequent lithostratigraphic interpretation results have shown that Permo-Carboniferous reservoir bearing formations are resolvable in numerous areas on good quality seismic. In addition, lithology and qualitative porosity interpretations are often possible.

The purpose of this paper is to review recent developments in the application of seismic lithostratigraphy to deep subsalt Permo-Carboniferous gas reservoirs in the Northwest German Basin (Figure 1). Modeling and interpretation results for selected objectives are presented, followed by a discussion of factors affecting lithostratigraphic interpretation and implications for exploration.

### PERMO-CARBONIFEROUS RESERVOIRS

The principal Permo-Carboniferous exploration objectives are the Upper Permian (Zechstein) dolomite and the Lower Permian (Rotliegendes) and Upper Carboniferous sandstones (Figure 2).

Manuscript received by the Editor July 24, 1989; revised manuscript received March 2, 1990.

\*Mobil Erdgas-Erdoel GmbH, P. O. Box 110, D3100, Celle, Federal Republic of Germany.

©1990 Society of Exploration Geophysicists. All rights reserved.

**Upper Permian (Zechstein) dolomite**

The Upper Permian dolomite occurs within the second of four Zechstein evaporite cycles in the Northwest German Basin. The dolomite has been subdivided into platform sebkha and tidal facies which grade basinward into shallow marine and finally deeper marine deposits, where a thickness greater than 200 m has been documented (Sannemann et al., 1978).

The reservoirs consist primarily of algal and crystalline dolomites. The algal dolomites are formed by both mud and grain-supported oncolites with variable amounts of mud. The crystalline dolomites, in contrast, consist of fine to

medium crystalline sucrosic dolomite with a noninterlocking texture. Core porosity, which commonly varies from 10 to 20 percent, may be as high as 30 percent. Petrographic observations indicate that most porosity is intergranular, but intragranular (dissolution) porosity also occurs in the algal dolomites. Variable amounts of anhydrite and calcite cement occur and are the main factors reducing porosity.

**Lower Permian (Rotliegendes) sandstones**

Several seismically resolvable reservoir sandstones are developed in the Lower Permian (Rotliegendes) where they

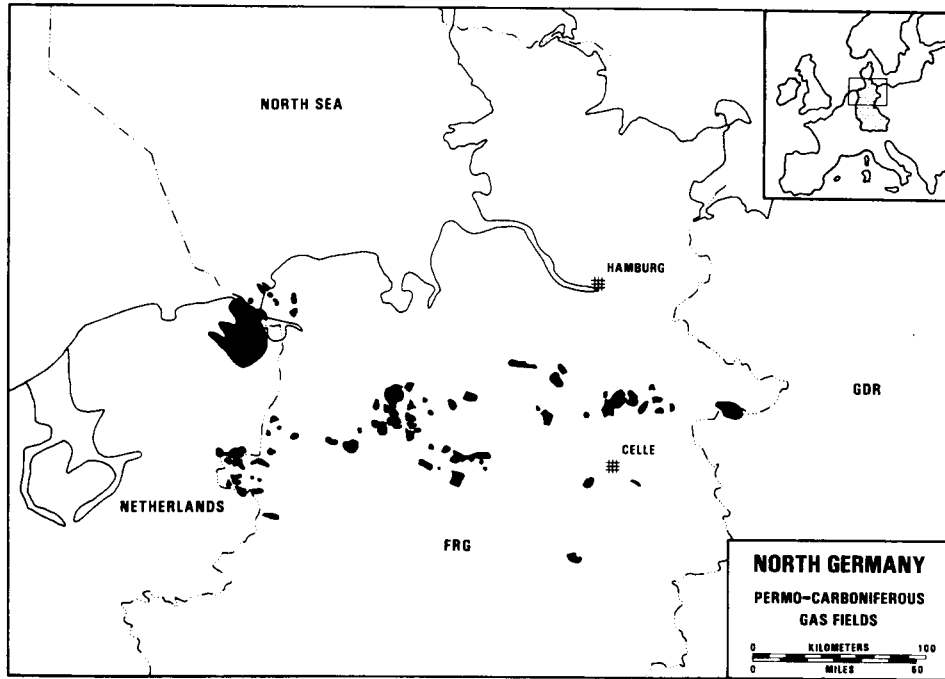


FIG. 1. Location of Permo-Carboniferous gas fields in the Northwest German Basin.

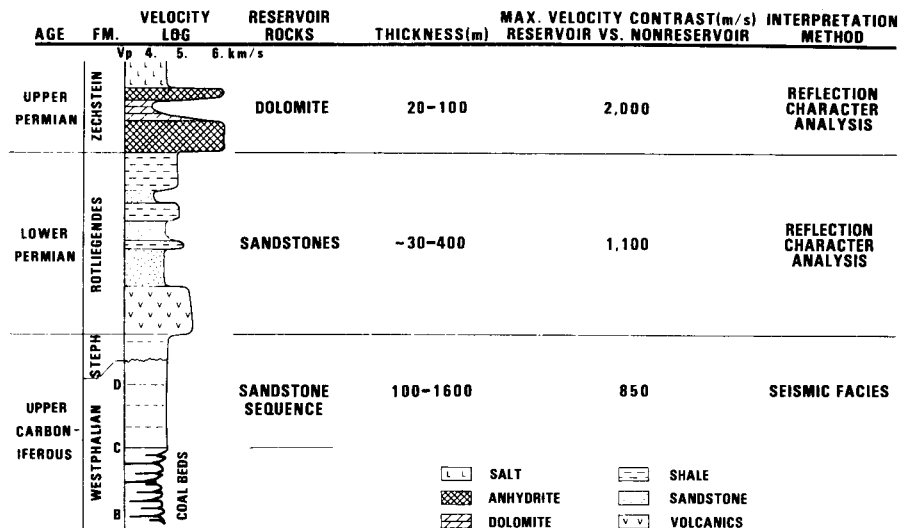


FIG. 2. Schematic velocity log (from sonic), thickness and velocity contrast of resolvable Permo-Carboniferous reservoirs, and corresponding stratigraphic interpretation method.

are interbedded with shales, conglomerates, breccias, and volcanics. The sandstones consist of subarkoses and sublitharenites deposited in predominantly aeolian and fluvial environments. Porosities, which are commonly 10 to 15 percent, may be as high as 22 percent. Porosity variations are controlled primarily by depositional environments. However, diagenetic events have also had a significant effect on porosity development and cementation (Drong, 1979). Thickness varies from a uniform 30–40 m along a shoreline-controlled sandstone belt to more than 400 m within Rotliegendes grabens.

### Upper Carboniferous sandstones

Upper Carboniferous sandstone reservoirs occur in the predominantly fluvial 3000 m thick Westphalian to Stephanian sequence. Westphalian B and Lower Westphalian C sandstones, which are interbedded with shales and thin coal beds, were deposited during humid conditions. A change to more arid conditions resulted in the deposition of an Upper Westphalian C, D, and Stephanian sequence which is generally devoid of coal beds (Hedemann and Teichmueller, 1971).

Sand distribution and reservoir quality vary both stratigraphically and areally. In general, the 800 m thick Westphalian C contains the best reservoir potential with a sandstone percentage up to 60 percent and porosities occasionally reaching 15 percent.

### LITHOSTRATIGRAPHIC MODELING AND INTERPRETATION

The Permian reservoirs are commonly greater than 20 m thick and are characterized by velocities 1100 m/s (sandstones) to 2000 m/s (dolomites) slower than the associated nonreservoir rocks (Figure 2). These reservoirs should be resolvable using reflection character analysis based on amplitude strength, signal characteristics, and interval time.

Underlying Upper Carboniferous sandstones often lack resolvable thickness or impedance contrasts between individual beds but may display larger scale seismic facies units. Since both Permian and Upper Carboniferous reservoirs can be seismically thin, frequency bandwidth is an important factor which must be considered.

Core porosity-sonic log crossplots (Figures 3a and 3b) illustrate that the interval transit time (slowness) of each formation increases with increasing porosity. The porosity-interval transit time relationship is consistent with the time average equation (Wyllie et al., 1956) calculated with matrix velocities of dolomites and quartz-rich sandstones compositionally similar to the Permo-Carboniferous reservoirs. This suggests that reservoir porosity variations may, in many cases, be correlated with seismic velocity, impedance, and reflection amplitudes.

### Upper Permian (Zechstein) dolomite

Within the Upper Permian sequence a series of high-amplitude reflections is commonly attributed to the large impedance contrast between low-impedance salt or saltclay and high-impedance anhydrites. 3-D zero-phase data acquired in 1985 display strong amplitude variations which correspond not only to these salt-anhydrite interfaces but to

pronounced porosity and thickness variations of the reservoir dolomites.

Lithostratigraphic modeling of selected wells and profiles was completed using impedance logs (derived from sonic and density logs) to determine if Permian dolomite porosity can be predicted. Maureau and van Wijhe (1979) demonstrated that high-porosity Zechstein 2 carbonates in The Netherlands have velocities low enough to produce pronounced reflections at the anhydrite-carbonate interface and that these reflections can be used to identify reservoir carbonates.

The effect of porosity variations on reflection character of a constant 45 m thick dolomite is illustrated in Figure 4a. A 5 percent porosity dolomite has an impedance similar to overlying and underlying anhydrites and is "seismically transparent." An increase in porosity to about 10 percent produces distinct reflections with a trough at the top and a peak at the base (zero-phase filter, reverse SEG polarity). Increasing porosities can be correlated with increasing amplitude strength. At 20 percent porosity, the dolomite produces amplitudes comparable with salt-anhydrite reflections (R.C. 0.30). The apparent thickening of the constant thick-

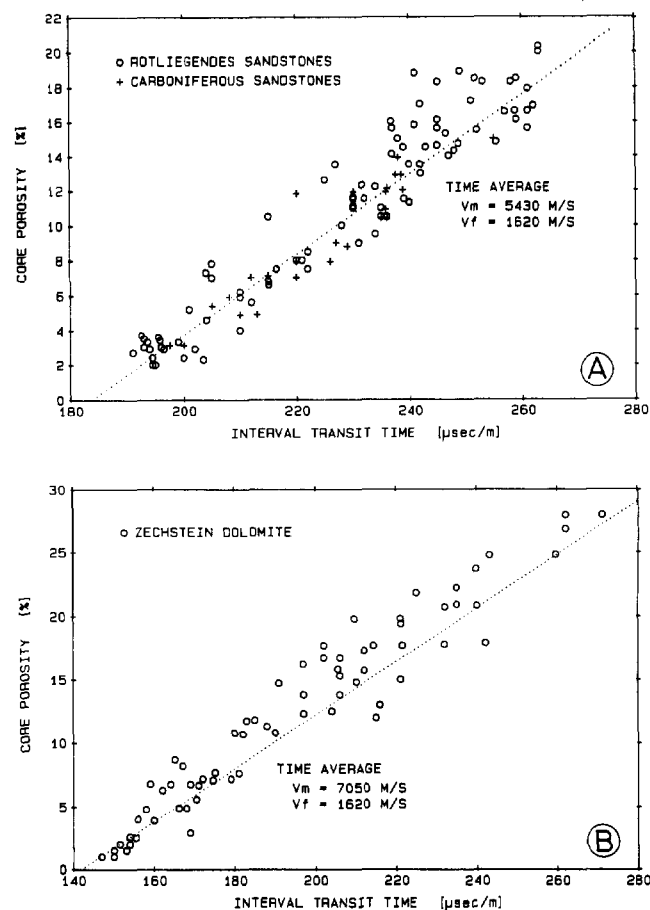


FIG. 3. Core porosity-sonic log crossplots illustrating reservoir rock porosity-velocity relationships in comparison with the time average equation (Wyllie et al., 1956; fluid velocity for 200 000 ppm brine).

ness layer is caused by the porosity-dependent velocity decrease (depth-time converted model).

The effect of thickness variations from 0–100 m on the reflection character of a constant porosity dolomite (~20 percent) is modeled in Figure 4b. Top and base reflections from the dolomite sequence interfere, producing amplitudes lower or higher than expected from the actual impedance contrast. The highest reflection amplitudes are caused by constructive interference of the top and base reflections between 35 and 45 m. Reflections from a thicker dolomite sequence (>80 m) are nearly constant in amplitude but simply farther apart in time.

In addition to porosity and thickness, other factors may influence Upper Permian dolomite reflection character. Since the dolomite is overlain by a relatively thin anhydrite (30–40 m), tuning of the anhydrite top and base reflection may influence reflection character. Care must be taken to evaluate possible tuning effects due to overlying anhydrite as well as dolomite thickness. Anhydrite-dolomite interbed multiples may also have a minor influence on base dolomite amplitudes, especially when dolomite porosities are high (high reflection coefficient).

In many prospective areas, Upper Permian dolomite thickness is commonly between 20 and 50 m. Therefore porosity and thickness variations cannot be clearly separated in the given frequency bandwidth. However, the presence of pronounced amplitudes beneath the salt-anhydrite reflection of the second cycle means that we must have sufficient dolomite porosity to cause reflections with overlying and underlying anhydrites. This suggests that dolomite

reflection amplitudes may be used as indicators of reservoir porosity.

Recently acquired 3-D data allow an interpretation of the dolomite reservoir quality throughout a large area. This 3-D data set is appropriate for lithostratigraphic interpretation for a variety of reasons: (1) uniform acquisition and processing, (2) poststack zero-phase transformation, (3) trace balancing with a large-window automatic gain control, and (4) spectral whitening to increase resolution.

The 3-D data display variable dolomite amplitudes (Figure 5) beneath the strong second-cycle salt-anhydrite reflection. High-amplitude reflections are caused by the porous dolomite facies. Ties with a discovery well zero-phase synthetic (Figure 5a) indicate that a pronounced trough and peak are produced by a 17 percent porosity dolomite reservoir sequence that is 29 m thick. Low-amplitude to “seismically transparent” zones beneath the salt-anhydrite peak are formed by low-porosity to tight dolomite facies as documented by the match with a synthetic seismogram from a dry hole with 7 percent porosity and 5 m net thickness (Figure 5b).

Lateral variations in Permian dolomite reservoir reflection amplitudes and porosity are clearly observable on numerous 3-D lines. The high-amplitude reflection tied to a porous dolomite facies (Figure 5a) displays a lateral decrease in amplitude to the east which is caused by a lower porosity dolomite facies. Increases in amplitude, on the other hand, also occur, indicating an increase in porosity.

The Permian dolomite reflection character and porosity interpretations were based on accurate delineation of the

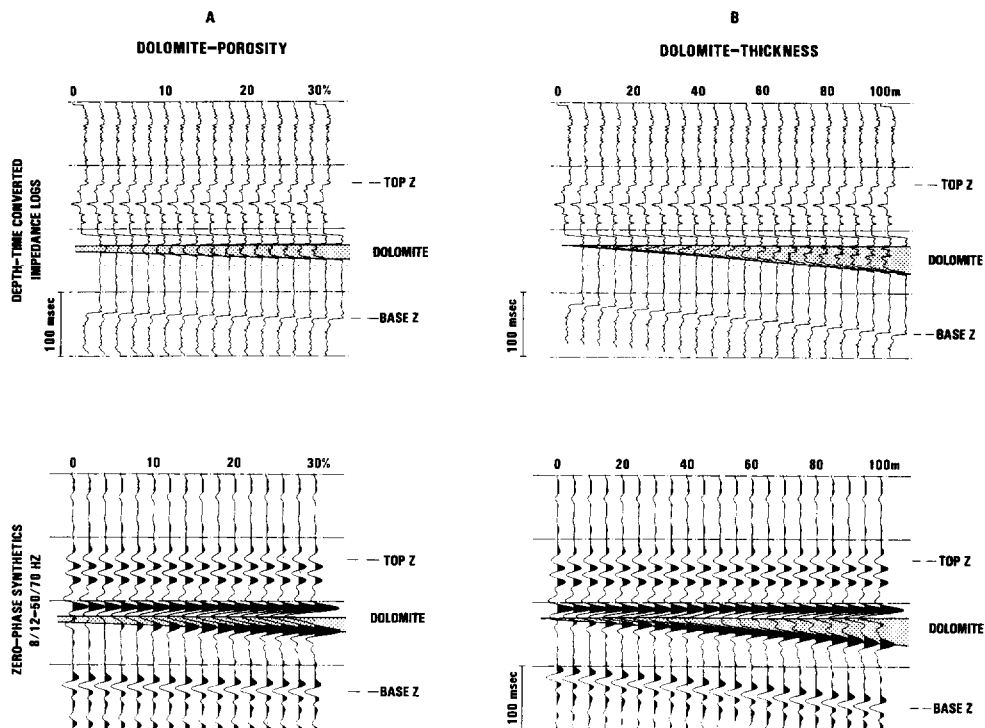


FIG. 4. Zechstein dolomite porosity (a) and thickness (b) modeling. The impedance, calculated from measured sonic and density logs, was modified by constant impedance shifts (a) and thickness modifications (b).

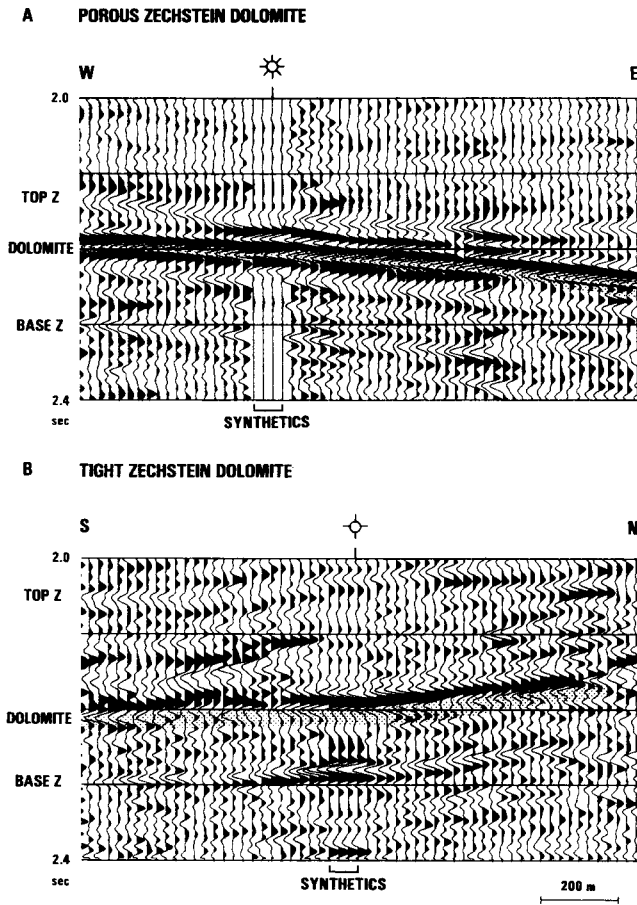


FIG. 5. High-amplitude porous dolomite reservoir (A) and low-amplitude tight reservoir facies (B) on selected lines from a 3-D seismic survey. Synthetic seismograms are plotted at each well location.

high-amplitude second cycle salt-anhydrite reflection. The overlying salt-anhydrite of the third cycle, where present, forms a high-amplitude reflection with the underlying shale-salt sequence (Figures 6a and 6b) which is similar to the reflections of a porous dolomite (Fig. 6c). Caution must be used since identification of the third-cycle anhydrite-salt reflection as the second-cycle anhydrite-porous dolomite interface could lead to incorrect interpretations of dolomite reservoir quality.

**Lower Permian (Rotliegendes) sandstones**

Lower Permian sandstones display large variations in thickness, porosity, velocity, and density. In many cases the porous reservoir sandstone impedance is significantly lower than the impedance of surrounding nonreservoir sandstones, shales, conglomerates, or volcanics and causes recognizable reflections. These reflections can be accurately modeled and interpreted given ties to well data and knowledge of the structural and stratigraphic setting which significantly reduces the number of interpretation possibilities.

**Thick sandstones.**—The discovery of a 300 m thick graben filling aeolian reservoir sandstone at the large Soehlingen gas field in 1980 (Drong et al., 1982) started a serious search for Early Permian grabens and thick graben filling reservoir sandstones. A reservoir sandstone with thickness variations from 25 to 115 m is modeled in Figure 7a (zero-phase filter, SEG polarity). At a discovery well, the porous sandstone (11.5 percent ~4150 m/s, 84 m net) is characterized at the top by a peak, followed by a lower amplitude trough and peak and then a slightly higher amplitude trough at the base. Thinning of the sandstones to 25 m will result in tuned top and bottom sandstone reflections. A high-amplitude peak-trough signal may therefore be indicative of a thin Lower Permian sandstone reservoir.

The effect of velocity (porosity) variations on the reflection character of a 115 m thick sandstone is also illustrated by Figure 7a. Nonreservoir sandstones with velocities of

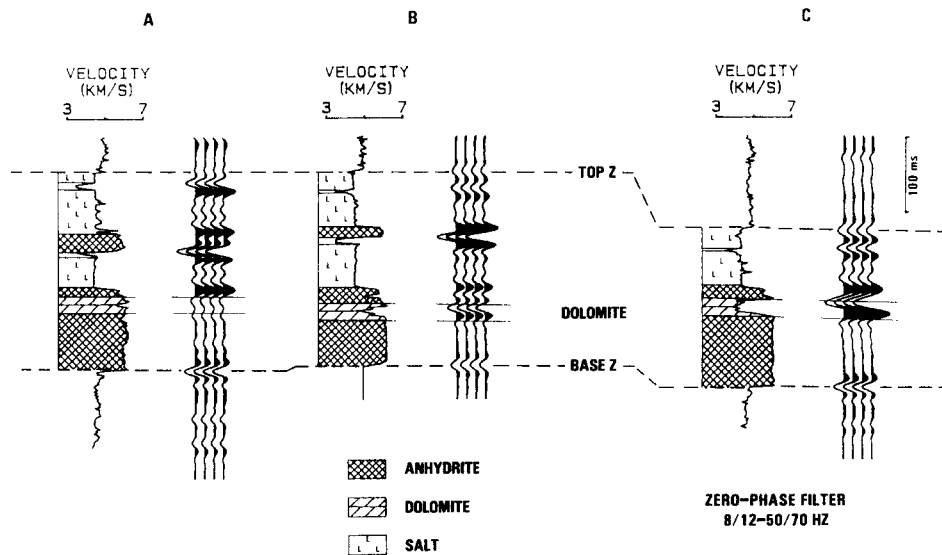


FIG. 6. Effect of anhydrite (third cycle) reflections on dolomite reflection character interpretation. High-amplitude anhydrite/salt reflections (a,b) can be easily confused with high-amplitude anhydrite/porous dolomite reflections (c).

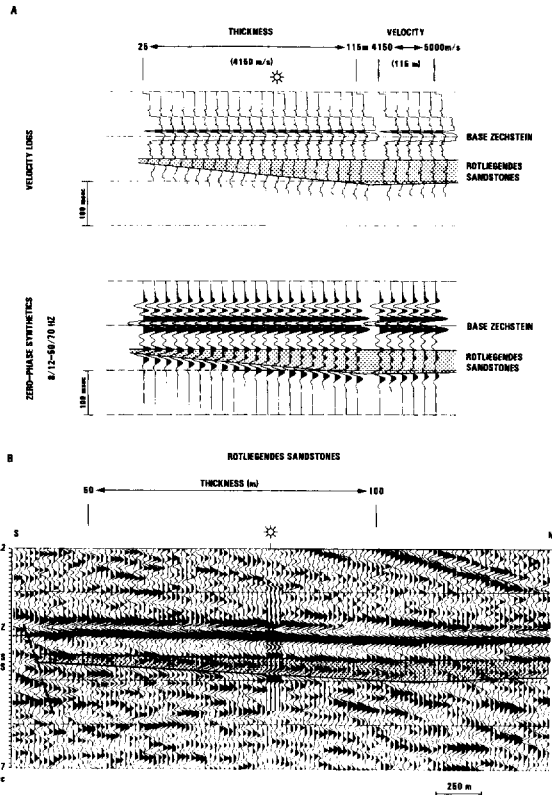


FIG. 7. Rotliegendes sandstone modeling of thickness and velocity variations (a) and interpretation of sandstone wedge on wavelet processed 2-D data (b).

about 5000 m/s do not display the higher amplitude reflections typical of reservoir sands with lower velocities.

A wavelet-processed 2-D seismic section is plotted in Figure 7b. Reflections tied to a discovery well zero-phase synthetic seismogram show a porous sandstone wedge from about 50 m to 100 m, as modeled in Figure 7a.

**Thin sandstones.**—At the southern rim of the Lower Permian basin an important reservoir sandstone has a relatively uniform thickness of 30–40 m. Reservoir porosity and net thickness, however, vary considerably due to changes in sedimentary facies and diagenetic cementation.

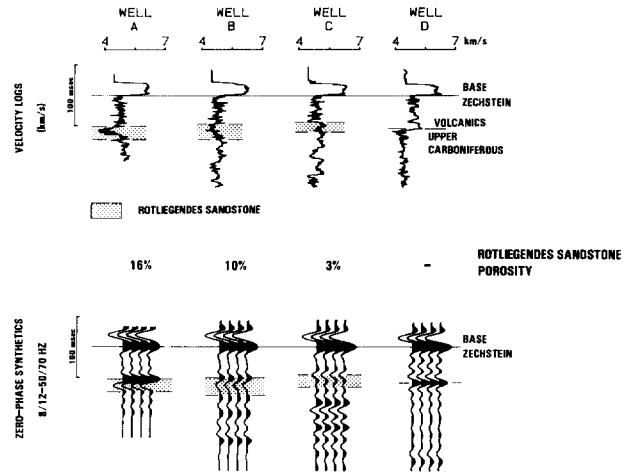


FIG. 8. Synthetic seismograms illustrating typical Rotliegendes sandstone reflection character variations with porosity (a–c) and similarity with Rotliegendes volcanics-Upper Carboniferous shale reflection (d).

Since total sandstone thickness does not vary significantly in the most prospective areas, porosity and net thickness variations are the dominant factors affecting reflection character. Synthetic seismograms from porous, low porosity and tight sandstones are displayed in Figure 8 to illustrate the effect of porosity on reflection character (Zero-Phase filter, SEG polarity). A high-porosity sandstone (16%) will produce pronounced top (peak) and base (trough) reflections (Figure 8a). Low porosity sandstone (10%), in contrast, will produce lower amplitude reflections (Figure 8b) while tight sands will be reflection-free or have low-amplitude reflections with the opposite polarity (Figure 8c).

Synthetic seismograms suggest that reflection amplitudes can be used to differentiate thin porous sandstones from lower porosity and tight sands. Caution needs to be used because, as illustrated by Figure 8d, reflections can be influenced or produced at the same depth by other geologic interfaces such as the Lower Permian volcanics-Upper Carboniferous interface.

Typical porosity-related amplitude variations are visible in

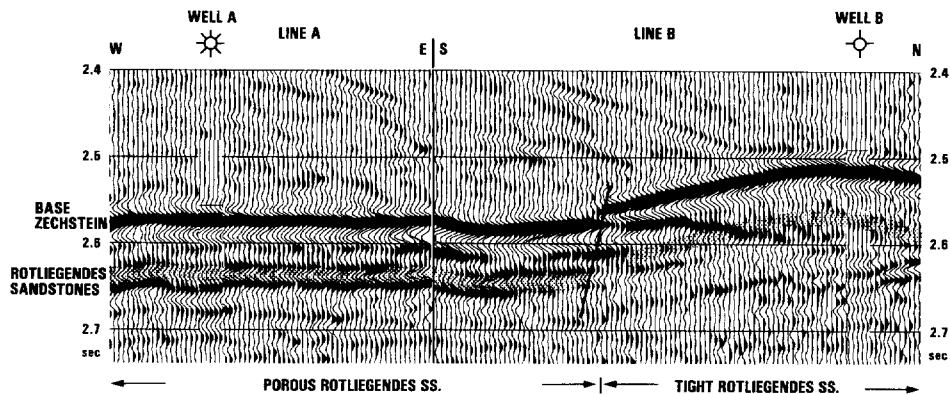


FIG. 9. Variation between porous high-amplitude (graben) and tight low-amplitude (horst block) Rotliegendes sandstone reflection character on a 2-D line.

Figure 9. Amplitudes from a 30 m (23 m net) thick sandstone vary from laterally continuous, high-amplitude reflections on the downthrown side of a fault to a low-amplitude or reflection-free-zone on the upthrown side. Well data indicate that a high-porosity (high-amplitude) reservoir facies (14.5 percent) was penetrated in the graben, whereas a nonreservoir facies (low amplitude) with porosities of about 3–7 percent was drilled on the horst block.

**Upper Carboniferous sandstones**

In contrast to resolvable Permian reservoirs, Upper Carboniferous reservoir sandstones from the Upper Westphalian C, D, and Stephanian are typically thin (<20 m) and lack significant velocity contrast with the nonreservoir silts and shales. Numerous low-velocity coal beds occur, however, in

the underlying Westphalian B-lower Westphalian C. Velocity and probable sedimentary facies variations suggest that larger scale seismic facies analysis may be useful for recognizing the Upper Westphalian C–D sequence with favorable reservoir properties.

Analysis of geologic data, modeling results, and seismic data indicates that the Upper Carboniferous can be divided into two seismic facies: a “continuous, high-amplitude” and a “discontinuous, low-amplitude” seismic facies (Figure 10). The continuous high-amplitude facies is caused by the constructive interference of reflections from thin (0.3–1 m), laterally continuous Westphalian B-Lower Westphalian C coal beds characterized by large impedance contrasts with overlying and underlying sediments. The low-amplitude discontinuous facies, in contrast, is produced by a sequence of Upper Westphalian C to Stephanian fluvial sandstones and shales which normally lack significant contrast in acoustic impedance.

The Upper Carboniferous seismic facies are clearly mappable on better quality seismic data (Figure 11). The facies contact is often gradational over several reflections but clearly shows the Carboniferous structure and the base of the prospective middle Westphalian C fluvial sediments. Thickness of the discontinuous low-amplitude facies can often be calculated whereas thickness of the underlying high-amplitude facies is difficult to interpret because the base of the facies is commonly obscured by multiples and noise.

**FACTORS AFFECTING LITHOSTRATIGRAPHIC INTERPRETATIONS**

Lithostratigraphic interpretation is dependent on the availability of high-quality wavelet-processed data with a large frequency bandwidth and real/relative amplitudes.

In the Northwest German Basin seismic lines were shot and processed over the last 20–30 years to gather additional

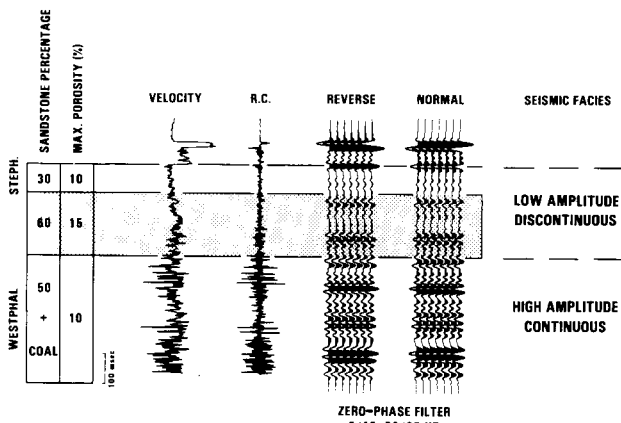


FIG. 10. Upper Carboniferous reservoir characteristics, log character, synthetic seismograms, and seismic facies.

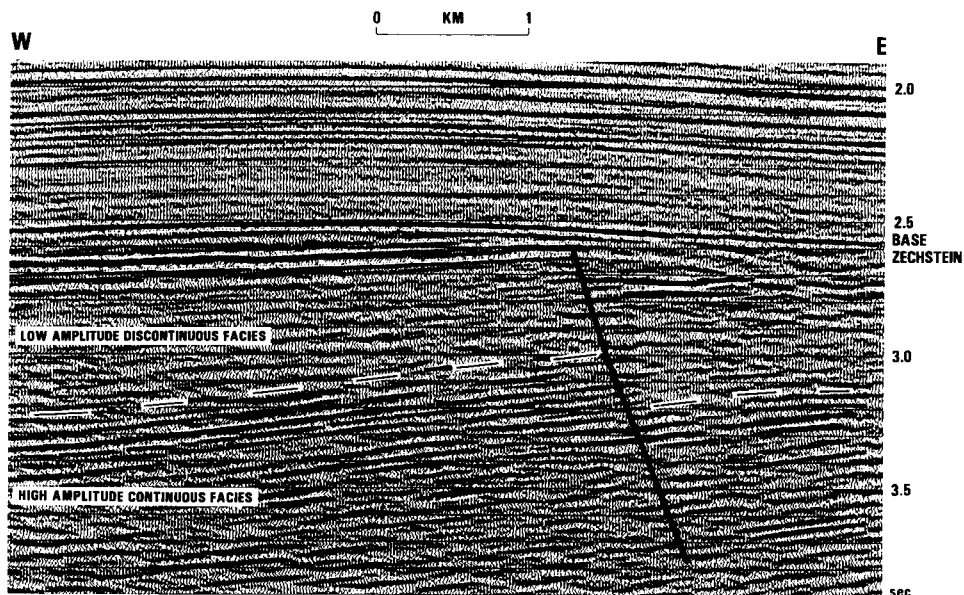


FIG. 11. Better quality Upper Carboniferous seismic displaying prospective low-amplitude discontinuous facies and underlying less prospective high-amplitude continuous facies.

2-D seismic information. Significant variations in acquisition and processing parameters occurred from year to year due to changes in equipment and interpretation objectives, and have resulted in a grid of variable vintage data which cannot be readily tied together.

A major factor influencing reflection character is the phase distortion by recording instrument filters and geophones. When combined with other factors significant phase variations commonly occur. As illustrated in Figure 12 (left), synthetic seismogram phase must be rotated a variable amount to match the phase shift of each intersecting 2-D

line. Modeling and interpretation difficulties with variable phase data can be reduced by applying the complementary phase angle to the seismic (Figure 12 right) to produce constant phase rotated displays that can be interpreted with zero-phase synthetics.

Spike deconvolution of dynamite data followed by zero-phase filtering is normally expected to produce zero-phase sections. However, distortion of the expected impulse (minimum-phase) wavelet by geophone response and instrument filters limits the effectiveness of spike deconvolution. To compensate for the distortion, instrument phase corrections

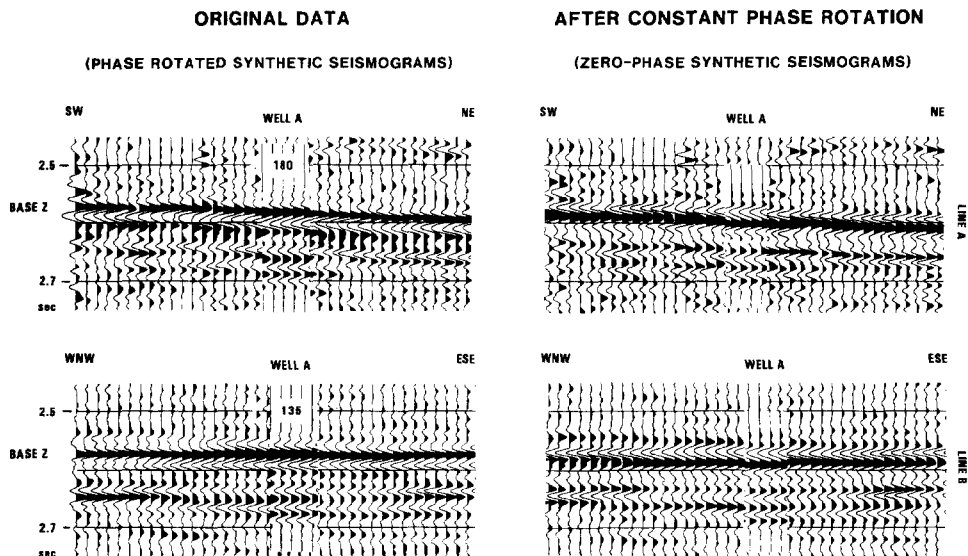


FIG. 12. Examples of variable vintage 2-D data with phase shift/time tie problems (left). Phase rotated zero-phase synthetics (180 degrees, 135 degrees) match the dynamite data. On the right side the complementary rotation angle was applied to the seismic data to compare with zero-phase synthetic seismograms.

ZERO-PHASE TRANSFORMATION  
LINE 87-A

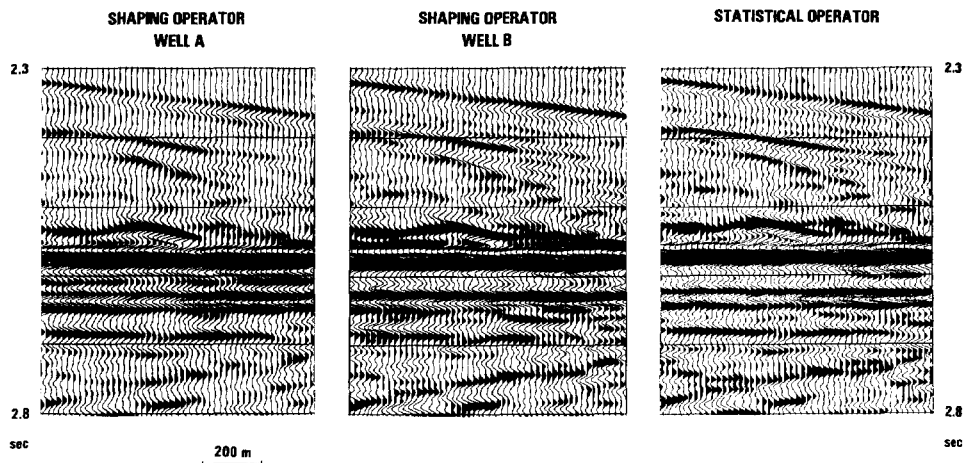


FIG. 13. Variability of zero-phase sections (same data window) which are processed with a shaping operator from wells A and B and a statistical operator, designed from the autocorrelation of the data.

(dephasing, minimum-phase transformation) need to be completed before spike deconvolution.

Since prestack phase corrections alone do not commonly compensate for all phase distortion (i.e., earth response), poststack zero-phase transformations with shaping operators derived from a reflectivity series or statistics (Redanz, 1988; Sheriff, 1980), or a constant phase shift (Levy and Oldenburg, 1987), are also necessary. Because zero-phase transformation results may be variable in quality, it is important to check the accuracy of the zero-phasing techniques with synthetic zero-phase seismograms.

Figure 13 gives an example of the variability of zero-phase transformations for the same data window. The only variation in processing is the choice of the zero phasing technique and operators, which are designed from the reflectivity series of wells A and B (shaping), or from the autocorrelation (statistics) of the given data set. Clear variations in reflection character and amplitude strength occur, especially in the window of interest (2.4–2.8). The variations indicate caution is needed to select the correct zero-phase version during detailed analysis of lithostratigraphy or the calculation of pseudoimpedance logs.

#### DISCUSSION

The increasing availability of wavelet-processed dynamite data should permit more accurate and routine lithostratigraphic interpretation of Northwest German Basin seismic data in the future. Comparison of the new Zechstein 3-D zero-phase data with older Netherlands seismic data previously used for reservoir interpretation (Mareau and Wijhe, 1979) documents the recent increases in resolution and the continuing trend from qualitative to quantitative interpretation.

Despite the improvements in data quality, important interpretation pitfalls remain and need to be considered during interpretation. Reflections with high amplitudes can be caused by not only porous dolomite and sandstone reservoirs, but by anhydrites, salt, volcanics, and coal beds. Interpretation needs to be completed with reference to nearby well control and appropriate geologic models.

High-amplitude reflections interpreted as porosity indicators may also be affected by a variety of other factors. Structural and geometrical effects such as focusing and defocusing can influence amplitude strength. Reflections may also display amplitude variations caused by velocity, thickness, and lateral continuity variations from overlying and underlying beds. Interference of reflections from laterally discontinuous Upper Permian anhydrites of the third cycle, for example, can cause lateral variations in Permian dolomite reflections. In general, the influence of these factors can be estimated and does not seriously limit interpretations of reservoir quality based on the occurrence of low-versus high-amplitude reflections.

In the northwestern German Basin where source rocks, traps, and seals are common, the ability to predict formation lithology and qualitative to quantitative porosity variations from deep subsalt seismic data should improve the drilling success ratio. When compared with the uncertainty of geologic porosity predictions from environmental and diagenetic relationships, lithostratigraphic interpretations of seismic data should increase confidence in the prediction of reservoir characteristics. The implications of these interpretations are important, not only for the northwestern German Basin, but also for the rest of northern Europe and other areas with subsalt reservoirs.

Lithostratigraphic interpretations should benefit not only exploration, but subsequent reservoir management. More accurate characterization and delineation of reservoirs with seismic data will provide a basis for more efficient development of reserves.

#### ACKNOWLEDGMENTS

We thank the management of Mobil Erdgas-Erdoel GmbH and concession partners BEB Erdgas-Erdoel GmbH, Texaco AG and Wintershall AG for permission to publish. Thanks are also due to J. D. McGehee for processing support, numerous exploration personnel for their assistance, G. Dion for typing, and J. Gundlach for drafting.

#### REFERENCES

- Drong, H. J., 1979, Diagenetische Veraenderungen in den Rotliegend Sandsteinen im NW-Deutschen Becken: *Zeit. der Deut. Geol. Gesellschaft*, **68**, 1172–1183.
- Drong, H. J., Plein, E., Sannemann, D., Schuepbach, M. A., and Zimbers, J., 1982, Der Schneverdinger Sandstein des Rotliegenden-eine aeolische Sedimentfuellung alter Grabenstrukturen: *Zeit. der Deut. Geol. Gesellschaft*, **133**, 699–725.
- Focht, G. W., and Baker, F. E., 1985, Geophysical case history of the Two Hills Colony gas field of Alberta: *Geophysics*, **50**, 1061–1076.
- Hedemann, H. A., and Teichmueller, R., 1971, Die palaeogeographische Entwicklung des Oberkarbons: *Fortschrittliche Geologie Rheinland und Westfalen*, **19**, 129–142.
- Levy, S., and Oldenburg, D. W., 1987, Automatic phase correction of common-midpoint stacked data: *Geophysics*, **52**, 51–59.
- Maureau, G. T. F. R., and van Wijhe, D. H., 1979, The prediction of porosity in the Permian (Zechstein 2) carbonate of eastern Netherlands using seismic data: *Geophysics*, **44**, 1502–1517.
- Redanz, M., 1988, Waveletextraktion und Inversion von Reflexionsseismogrammen zur Ableitung von akustischen Impedanzen: *Berichte des Instituts für Geophysik der Ruhr-Universität Bochum*, Reihe A, no. 25.
- Sannemann, D., Zimdars, J., and Plein, E., 1978, Der basale Zechstein (A2 - T1) zwischen Weser und Ems: *Zeit. der Deut. Geol. Gesellschaft*, **121**, 33–69.
- Schott, W., 1982, Crude oil and natural gas in the Federal Republic of Germany: development and prospects: *J. Petr. Geol.*, **3**, 235–266.
- Schroeder, L., 1986, Erdoel und Erdgasexploration in der Bundesrepublik Deutschland 1986: *Erdoel, Erdgas, Kohle*, **103**, 314–324.
- Sheriff, R. E., 1980, *Seismic stratigraphy*: Internat. Human Res. Dev. Corporation.
- Wyllie, M. R. J., Gregory, A. R., and Gardner, L. W., 1956, Elastic wave velocities in heterogeneous and porous media: *Geophysics*, **21**, 41–70.